JOURNAL OF BACTERIOLOGY, Mar. 1996, p. 1631–1639 Vol. 178, No. 6
0021-9193/96/$04.00+0

The *Myxococcus xanthus rfbABC* Operon Encodes an ATP-Binding Cassette Transporter Homolog Required for O-Antigen Biosynthesis and Multicellular Development

DONGCHUAN GUO, M. GABRIELA BOWDEN, RASHMI PERSHAD,† AND HEIDI B. KAPLAN*

Department of Microbiology and Molecular Genetics, The University of Texas Medical School, Houston, Texas 77030

Received 27 September 1995/Accepted 29 December 1995

A wild-type *sasA* locus is critical for *Myxococcus xanthus* multicellular development. Mutations in the *sasA* locus cause defective fruiting body formation, reduce sporulation, and restore developmental expression of the early A-signal-dependent gene 4521 in the absence of A signal. The wild-type *sasA* locus has been located on a 14-kb cloned fragment of the *M. xanthus* chromosome. The nucleotide sequence of a 7-kb region containing the complete *sasA* locus was determined. Three open reading frames encoded by the genes, designated *rfbA*, *B*, and *C* were identified. The deduced amino acid sequences of *rfbA* and *rfbB* show identity to the integral membrane domains and ATPase domains, respectively, of the ATP-binding cassette (ABC) transporter family. The highest identities are to a set of predicted ABC transporters required for the biosynthesis of lipopolysaccharide O-antigen in certain gram-negative bacteria. The *rfbC* gene encodes a predicted protein of 1,276 amino acids. This predicted protein contains a region of 358 amino acids that is 33.8% identical to the *Yersinia enterocolitica* O3 *rfbH* gene product, which is also required for O-antigen biosynthesis. Immunoblot analysis revealed that the *sasA1* mutant, which was found to encode a nonsense codon in the beginning of *rfbA*, produced less O-antigen than *sasA*$^+$ strains. These data indicate that the *sasA* locus is required for the biosynthesis of O-antigen and, when mutated, results in A-signal-independent expression of 4521.

Multicellular development of *Myxococcus xanthus* is orchestrated by numerous extracellular signals (7, 15), including one of the earliest signals, A signal. The *M. xanthus* developmental cycle is initiated when this gram-negative soil bacterium is starved at a high cell density. The cells aggregate into organized mounds, termed fruiting bodies, within which the originally rod-shaped cells differentiate into environmentally resistant ovoid spores. This developmental program ensures the survival of the organism until nutrients are restored and the spores can germinate (8, 37).

Extracellular A signal allows the cells to sense their cell density (25). The A signal is composed of a specific subset of amino acids which can function either individually or in combination at a concentration greater than 10 μM (24). The A signal appears to be generated when proteinases, released in response to nutrient limitation, degrade surface proteins to their constituent amino acids and peptides (24, 32). If the cells are at a density of greater than about 3×10^8/ml, the concentration of extracellular amino acids and peptides exceeds the critical threshold concentration of 10 μM and the A-signal-dependent developmental genes are expressed (25). Two genes known to be involved in the generation of A signal are *asgA* and *asgB*, which encode domains of a fused two-component environmental sensor and response regulator (33) and a putative DNA-binding protein (31), respectively.

Response to extracellular A signal can be measured by the expression of the earliest A-signal-dependent gene isolated to date. This gene is designated 4521 in reference to the Tn*5 lac* Ω4521 transposon inserted in the gene (21). Expression of 4521 in wild-type cells begins to increase at 1 to 2 h after the initiation of development (21, 23). Expression of 4521, as measured by Northern (RNA blot) analysis and β-galactosidase activity, is at basal levels in all of the *asg* backgrounds (17, 23, 33). This expression can be restored by the addition of exogenous A signal (23) or the presence of the *sasA* or *sasB* suppressor mutations (17).

Control of 4521 expression is complex. Developmental expression requires both high cell density and nutrient limitation (17, 25). Each condition appears to control 4521 expression independently (17, 40). The 4521 promoter has recently been identified as a member of the sigma 54 family (19). This is based on evidence including the presence of a "−12 and −24" consensus sequence (19) and the requirement for the region starting between 125 and 146 bp upstream of the transcription start site for full 4521 developmental expression (14). It is expected that 4521, similar to other sigma 54-dependent genes, will require at least one activator to bind to the region upstream of the promoter for open complex formation (26).

The *sasA* and *sasB* suppressor mutations were isolated in a genetic screen to identify negative regulators in the pathway linking the exogenous A signal to its responsive gene, 4521. Specifically, the *asgB480* parent strain containing Tn*5 lac* Ω4521, which is Lac$^-$ on nutrient and starvation plates, was mutagenized with UV light and plated on nutrient agar. The resulting Lac$^+$ colonies were isolated, and their mutations were mapped to the *sasA* and *sasB* loci (17).

The *sasA* locus is particularly interesting because a wild-type *sasA* locus is required for normal development. The *sasA* mutant alleles, when present in an otherwise wild-type background, result in delayed aggregation, abnormal fruiting body formation, and reduced sporulation. In addition, the *sasA* mutations restore 4521 expression to the *asgB* parent during early

* Corresponding author. Mailing address: Department of Microbiology and Molecular Genetics, The University of Texas Medical School, 6431 Fannin, Houston, TX 77030. Phone: (713) 794-1744. Fax: (713) 794-1782. Electronic mail address: hkaplan@utmmg.med.uth.tmc.edu.

† Present address: Department of Molecular Genetics, The University of Texas M.D. Anderson Cancer Center, Houston, TX 77030.

development in a pattern that is wild type with respect to expression level and timing. The vegetative phenotypes of reduced colony diameter, glossy colony surface, and reduced cohesiveness are also characteristic of *sasA* mutants (17).

We report here the cloning, sequencing, and functional analysis of the *sasA* locus. This locus encodes three genes, designated *rfbA*, *B*, and *C*, which are homologous to the *rfb* genes of certain other gram-negative bacteria (3, 20, 44, 49). We have determined that these *M. xanthus rfb* genes function in O-antigen biosynthesis and, when mutated, result in A-signal-independent developmental expression of 4521.

MATERIALS AND METHODS

Bacterial strains, plasmids, culture conditions, and growth media. The bacterial strains and plasmids used in this study are listed in Table 1. The *M. xanthus* recipient strains DK6600 and DK6621 contain a Tn*5 lac* Ω4521 (Tc^r) insertion (17) to monitor 4521 expression. Strain DK6600 is deficient in the generation of A signal as a result of the *asgB480* mutation. Strain DK6621 carries *asgB480* and the *sasA1* mutant allele, which restores 4521 developmental expression. Strain DK6620 was used as the wild type because the Ω4521 insertion does not appear to alter any growth or developmental functions. *M. xanthus* strains were grown at 32°C in CTT liquid medium with vigorous shaking or on CTT agar (14). Kanamycin (40 μg/ml) or oxytetracycline (12.5 μg/ml) was added when appropriate. The growing cells were used in the mid-exponential phase (80 to 160 Klett units, which is approximately 4×10^8 to 8×10^8 cells per ml). The *Escherichia coli* strains were grown at 37°C in LB liquid medium (35) or on LB agar (LB liquid with 1.5% Bacto-Agar [Difco Laboratories]), which both contained ampicillin (100 μg/ml) or kanamycin (50 μg/ml) when appropriate to maintain plasmids.

Plasmid constructions. The vector pHBK429 was constructed as an in situ cloning vector. It is a derivative of pREG429 constructed by R. Gill (13) in which the P1 incompatibility region has been omitted. This vector must be transferred into *M. xanthus* by electroporation. To construct pHBK429, the 2.9-kb *Eco*RI-*Sal*I fragment of pREG429 containing part of the tetracycline resistance gene of pBR322 and part of the transposon Tn*5* ($IS50_L$ through to the *Sal*I site in the internal region) was ligated to pUC18 (48) digested with *Eco*RI and *Sal*I. The vector pHBK429 was prepared from the appropriate ampicillin- and kanamycin-resistant *E. coli* MC1061 transformants. Plasmid pHBK400 was constructed as described in the Results. Other plasmids in the 400 series were constructed as described in Table 1. The protocols used, such as plasmid isolation, restriction endonuclease digestion, ligation in low-melting-point agarose, and other standard molecular biological techniques, are from Sambrook et al. (35).

Plasmid transfer to *M. xanthus*. The plasmids were transferred from *E. coli* to *M. xanthus* by electroporation using the original method developed by J. Rodriguez (22) or a modification of that method (18).

DNA sequence and computer analysis. The DNA sequence of the 7-kb region containing the *sasA* locus was determined. The sense and antisense strands were each sequenced at the DNA Core Facility of the Department of Microbiology and Molecular Genetics with an ABI 373A DNA Sequencer (Perkin Elmer, Applied Biosystems Division) using *Taq* polymerase in a thermal cycling reaction. The sequence of the 4-kb *Sac*I fragment was confirmed by manual sequencing of the sense strand with the Sequenase version 2 DNA sequencing kit (United States Biochemical) by the Sanger et al. dideoxy method (36). The double-stranded template DNA was prepared by the alkaline lysis method, the Magic Miniprep DNA purification system (Promega), and the QIAprep Spin kit (Qiagen). The T3, T7, and −20 primers were used.

The 4-kb *Sac*I fragment was sequenced primarily with derivatives of pHBK440 and pHBK450 generated with the double-stranded nested deletion kit (Pharmacia LKB). Certain modifications of the protocol were made. First, the plasmids were digested with *Sac*I and then *Eco*RI and incubated with exonuclease III at 37°C in the absence of NaCl. Samples were removed each minute for 20 min, treated with S1 nuclease, and then combined into one tube. This combined sample was incubated with the Klenow fragment of DNA polymerase I and 0.2 mM deoxynucleoside triphosphates (dNTPs) to ensure blunt ends. *Eco*RI linkers were ligated to the ends to allow the inserts to be easily removed. To eliminate extra linkers, the sample was digested with *Eco*RI and electrophoresed through low-melting-point agarose. The agarose containing DNA in the desired size range (3 to 7 kb) was excised in 10 portions of different-sized DNA fragments. Each portion was diluted, ligated, and transferred into *E. coli* DH5α. Plasmid DNA was prepared from the transformants and digested with *Eco*RI and *Hin*dIII to identify the plasmids with inserts of the appropriate size for sequencing. Regions not sequenced with the exonuclease III-generated plasmids were sequenced with subclones.

The DNA sequences were aligned and edited with the SeqEd 675 DNA sequence editor program (Perkin Elmer, Applied Biosystems Division). The University of Wisconsin Genetic Computer Group's (GCG) sequence software package, version 8.0 (6), was used for sequence analysis. The Codonpreference program predicted the open reading frames based on the G-C codon bias of the third position in this high (67.5%) G+C organism (6). The Tfasta program searched the GenBank and EMBL databases for sequence identities. Searches were also performed at the National Center for Biotechnology Information with the BLAST network service (1). The Pileup program aligned the protein sequences. The Bestfit program determined pairwise identities. The Motifs program identified motifs common to ATP-binding proteins in *M. xanthus* RfbB.

Identification of the *sasA1* mutation. To identify the DNA alteration causing the *sasA1* mutation, PCR products of the region containing the mutation were cloned and sequenced. Since the *sasA1* mutation mapped roughly to the region corresponding to the middle of the 1.5-kb *M. xanthus* DNA insert in pHBK402, two primers estimated to flank the mutation were designed. The sequence of primer 1 is 5′-AGGAGCTCTGGGAAGCCAGGGG-3′. The sequence of primer 2 is 5′-GGAGAACCAGATCCACGG-3′. These primers are composed of wild-type sequences from bp 670 to 686 and bp 1095 to 1078, respectively. PCR was performed in a GeneAmp PCR system 2400 (Perkin Elmer) for 30 cycles under the following conditions: 94°C for 30 s, 55°C for 30 s, and 72°C for 50 s. Two identical reactions contained 50 to 100 ng of chromosomal DNA of the *sasA1 asgB480* mutant DK6621, 1 pmol of each primer, 2 mM $MgCl_2$, 0.2 mM dNTPs, and 3 U of *Taq* polymerase (Promega) in a total volume of 50 μl. The 425-bp PCR products from these reactions were cloned into the *Hin*dIII and *Sac*I sites of pBluescript KS (Stratagene). The sequence of both strands of one plasmid from each reaction was determined as described above with T3 and T7 primers.

Immunoblot analysis. Mid-logarithmic-phase *M. xanthus* cells (3×10^7 to 5×10^7) were harvested, washed in 10-fold excess TBS buffer (200 mM Tris-HCl, 500 mM NaCl, pH 7.5), and resuspended in the same buffer at 5×10^7 cells per ml. The cells (5×10^6 per slot) were placed onto a Nitro ME transfer membrane (Micron Separations, Inc.) with a Bio-Dot SF microfiltration unit (Bio-Rad). The membrane was immersed in 2% gelatin in TBS for 1 h at room temperature and then washed for 5 min in TBS. This membrane was divided into six identical pieces, and each piece was immersed in the appropriate monoclonal antibody (MAb) diluted 1:2,000 in TBS and incubated overnight at room temperature. The membranes were washed together four times for 6 min in TTBS (TBS buffer containing 0.05% Tween 20). Next, the membranes were immersed for 1 h in goat anti-mouse immunoglobulin G (IgG)-alkaline phosphatase conjugate (Promega) diluted 1:7,000 in TBS at room temperature. The membranes were washed four times for 6 min in TTBS and then for 5 min in TBS. Finally, the 5-bromo-4-chloro-3-indolylphosphate and nitroblue tetrazolium substrates (Bio-Rad) were added, and the membranes were incubated at room temperature for 10 to 30 min until adequate color development was observed.

A-signal activity. The A-signal assay was performed as described by Kuspa and Kaiser (22).

Nucleotide sequence accession number. The nucleotide sequence of the *sasA* locus has been assigned GenBank accession number U36795.

RESULTS

In situ cloning of the *sasA* locus. To clone the wild-type *sasA* locus from the *M. xanthus* chromosome, the in situ cloning method developed by R. Gill (13) was used. In this method, a vector integrates into a Tn*5* in the chromosome, providing an *E. coli* origin of replication and restriction sites for cloning adjacent DNA. Specifically, the newly constructed vector, pHBK429, was electroporated into strain DK6640, which contains Tn*5* Ω6636(Tc^r) linked to the wild-type *sasA* locus. Southern analyses of 10 resulting HK1049 strains confirmed the integration of the plasmid in each of two different orientations and mapped the location of various restriction sites in the area. Chromosomal DNA from these 10 strains was purified, pooled, digested with *Eco*RI, ligated, and transferred into *E. coli* MC1061. A 19-kb plasmid, pHBK400, was purified from one of the resulting colonies.

The 14-kb fragment of the *M. xanthus* chromosome carried on pHBK400 contains the wild-type *sasA* locus, which is dominant over the mutant *sasA1* allele in a heterozygotic tandem duplication. This was shown by the ability of pHBK400 to restore the SasA$^+$ phenotype to a *sasA* mutant when electroporated into DK6621, the *sasA1 asgB480* mutant. The resulting *M. xanthus* transformants, strains HK1050, were overlaid with 0.04% 5-bromo-4-chloro-3-indolyl-β-D-galactopyranoside (X-Gal), the chromogenic substrate of β-galactosidase. Seventy-nine percent of the transformants (779 of 985) were SasA$^+$ (tan colonies identical to the *asgB480* parent). These tan colonies had a wild-type diameter and surface morphology. Twenty-one percent of the transformants were SasA$^-$ (small glossy

TABLE 1. Plasmid and strain list

Plasmid or strain	Relevant characteristics	Source, reference, or construction
Plasmids		
pBluescript KS$^+$	Amp^r	Stratagene
pREG429	Kan^r	13
pUC18	Amp^r	48
pHBK429	Kan^r	2.9-kb *Eco*RI-*Sal*I fragment of pREG429 ligated into pUC18
pBGS18	Kan^r	41
pLJS49	Kan^r, P1 inc, *M. xanthus* Mx8 phage ATT site	38
pYC274	Kan^r, *M. xanthus* Mx8 phage ATT site	2.8-*Sma*I fragment of the *M. xanthus* Mx8 phage ligated with *Dra*I-digested pBGS18 (C. Yang)
pHBK400	Kan^r	14-kb insert containing the *sasA* locus resulting from ligation of *Eco*RI-digested chromosomal DNA of 10 pooled HK1049^a strains
pHBK401	Kan^r, fragment 1	8-kb *Mlu*I fragment from pHBK400 ligated into the *Sma*I site of pBGS18
pHBK402	Kan^r, fragment 2	1.5-kb *Nco*I fragment from pHBK400 ligated into the *Sma*I site of pBGS18
pHBK404	Kan^r, fragment 4	4-kb *Sac*I fragment from pHBK400 ligated into pBGS18
pHBK405	Kan^r, fragment 5	1.3-kb *Pst*I fragment from pHBK400 ligated into pBGS18
pHBK406	Kan^r, fragment 6	2-kb *Nco*I fragment from pHBK400 ligated into pBGS18
pHBK407	Kan^r, fragment 7	5.3-kb *Pst*I-*Sal*I fragment from pHBK400 ligated into pBGS18
pDG408	Kan^r, fragment 8	1.9-kb *Eag*I fragment from pHBK407 ligated into the *Sma*I site of pBGS18
pDG409	Kan^r, fragment 9	1.2-kb *Apa*I fragment from pHBK407 ligated into the *Sma*I site of pBGS18
pDG410	Kan^r, fragment 10	1.2-kb *Sph*I fragment from pHBK407 ligated into pBGS18
pHBK421	Kan^r, fragment 1, *M. xanthus* Mx8 phage ATT site	8-kb *Eco*RI-*Hin*dIII fragment from pHBK401 ligated into pLJS49
pHBK422	Kan^r, fragment 2, *M. xanthus* Mx8 phage ATT site	1.5-kb *Eco*RI-*Hin*dIII fragment from pHBK402 ligated into pLJS49
pDG423	Kan^r, fragment 3, *M. xanthus* Mx8 phage ATT site	2-kb *Sac*I-*Bss*HII fragment from pHBK450 ligated with *Hin*dIII-*Sma*I-digested pYC274
pHBK424	Kan^r, fragment 4, *M. xanthus* Mx8 phage ATT site	4-kb *Eco*RI-*Hin*dIII fragment from pHBK404 ligated into pLJS49
pHBK427	Kan^r, fragment 7, *M. xanthus* Mx8 phage ATT site	5.3-kb *Eco*RI-*Hin*dIII fragment from pHBK407 ligated into pLJS49
pHBK440	Amp^r, fragment 4	4.0-kb *Sac*I fragment from pHBK400 ligated into the *Eco*RV site of pBluescript KS$^+$ (orientation I)
pHBK450	Amp^r, fragment 4	4.0-kb *Sac*I fragment from pHBK400 ligated into the *Eco*RV site of pBluescript KS$^+$ (orientation II)
E. coli		
DH5α	*supE44ΔlacU169* (ϕ80*lacZ*ΔM15 *hsdR17 recA1 endA1 gyrA96 thi-1 relA1*)	16
MC1061	*hsdR mcrB araD139*Δ(*araABC-leu*)*7679ΔlacX74 galU galK rpsL thi*	4
M. xanthus		
DK6600	Tn*5 lac* Ω4521(Tc^r) *sglA1 asgB480*	17
DK6620	Tn*5 lac* Ω4521(Tc^r) *sglA1*	17
DK6621	Tn*5 lac* Ω4521(Tc^r) *sglA1 asgB480 sasA1*	17
DK6638	Tn*5* Ω6636(Kan^r) *sglA1*	17
DK6639	Tn*5* Ω6636(Kan^r) *sglA1 sasA1*	17
DK6640	Tn*5* Ω6636(Tc^r) *sglA1*	17
DK6641	Tn*5* Ω6636(Tc^r) *sglA1 sasA1*	17
HK1049^a	Tn*5* Ω6636(Tc^r) *sglA1* pHBK429	Introduction of pHBK429 into DK6640 by electroporation
HK1050	*sasA* merodiploid, Tn*5 lac* Ω4521(Tc^r) *sglA1*	Introduction of pHBK400 into DK6600 by electroporation
HK1052	*sasA* merodiploid, Tn*5 lac* Ω4521(Tc^r) *sglA1*	Introduction of pHBK402 into DK6600 by electroporation
HK1055	*sasA* merodiploid, Tn*5 lac* Ω4521(Tc^r) *sglA1*	Introduction of pHBK405 into DK6600 by electroporation
HK1056	*sasA* merodiploid, Tn*5 lac* Ω4521(Tc^r) *sglA1*	Introduction of pHBK406 into DK6600 by electroporation
HK1058	*sasA* merodiploid, Tn*5 lac* Ω4521(Tc^r) *sglA1*	Introduction of pDG408 into DK6600 by electroporation
HK1059	*sasA* merodiploid, Tn*5 lac* Ω4521(Tc^r) *sglA1*	Introduction of pDG409 into DK6600 by electroporation
HK1060	*sasA* merodiploid, Tn*5 lac* Ω4521(Tc^r) *sglA1*	Introduction of pDG410 into DK6600 by electroporation
HK1061	*sasA* merodiploid, Tn*5 lac* Ω4521(Tc^r) *sglA1 asgB480 sasA1*	Introduction of pHBK401 into DK6621 by electroporation
HK1062	*sasA* merodiploid, Tn*5 lac* Ω4521(Tc^r) *sglA1 asgB480 sasA1*	Introduction of pHBK402 into DK6621 by electroporation
HK1065	*sasA* merodiploid, Tn*5 lac* Ω4521(Tc^r) *sglA1 asgB480 sasA1*	Introduction of pHBK405 into DK6621 by electroporation
HK1066	*sasA* merodiploid, Tn*5 lac* Ω4521(Tc^r) *sglA1 asgB480 sasA1*	Introduction of pHBK406 into DK6621 by electroporation
HK1067	*sasA* merodiploid, Tn*5 lac* Ω4521(Tc^r) *sglA1 asgB480 sasA1*	Introduction of pHBK407 into DK6621 by electroporation
HK1071	*sasA* merodiploid, Tn*5 lac* Ω4521(Tc^r) *sglA1 asgB480 sasA1*	Introduction of pHBK421 into DK6621 by electroporation
HK1072	*sasA* merodiploid, Tn*5 lac* Ω4521(Tc^r) *sglA1 asgB480 sasA1*	Introduction of pHBK422 into DK6621 by electroporation
HK1073	*sasA* merodiploid, Tn*5 lac* Ω4521(Tc^r) *sglA1 asgB480 sasA1*	Introduction of pDG423 into DK6621 by electroporation
HK1074	*sasA* merodiploid, Tn*5 lac* Ω4521(Tc^r) *sglA1 asgB480 sasA1*	Introduction of pHBK424 into DK6621 by electroporation
HK1077	*sasA* merodiploid, Tn*5 lac* Ω4521(Tc^r) *sglA1 asgB480 sasA1*	Introduction of pHBK427 into DK6621 by electroporation

^{a} A pool of 10 different HK1049 strains with pHBK429 integrated into the chromosome in different orientations was used to prepare chromosomal DNA for the in situ cloning of pHBK400.

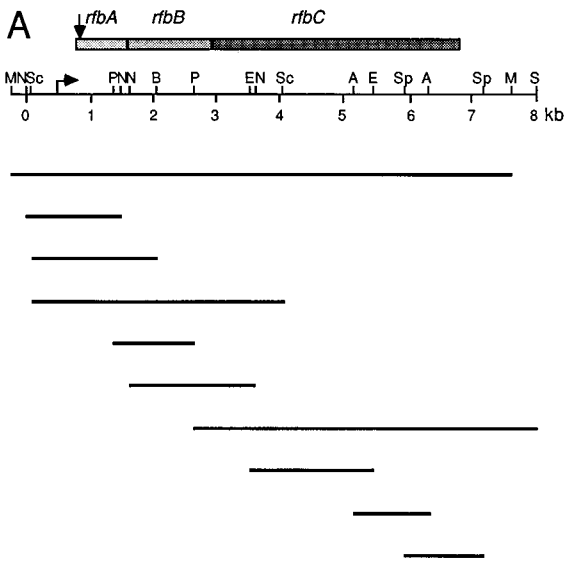

B

Plasmids	% SasA+ transformants: Integration site: *sasA* (Strain background: *asgB*)	*sasA* (*asgBsasA1*)	ATT (*asgBsasA1*)
pHBK401 pHBK421	ND	83.6	100
pHBK402 pHBK422	100	49.9	<0.1
pHBK423	ND	ND	100
pHBK424	ND	ND	100
pHBK405	1.1	<0.2	ND
pHBK406	1.6	2.3	ND
pHBK407 pHBK427	ND	<0.1	<0.2
pHBK408	<0.3	ND	ND
pHBK409	<0.4	ND	ND
pHBK410	100	ND	ND

FIG. 1. Genetic analysis of the *sasA* locus. (A) Physical map of the *sasA* locus. ORFs are represented by shaded boxes. The vertical arrow indicates the location of the *sasA1* mutation. Restriction enzyme abbreviations: A, *Apa*I; B, *Bss*HII; E, *Eag*I; M, *Mlu*I; N, *Nco*I; P, *Pst*I; S, *Sal*I; Sc, *Sac*I; Sp, *Sph*I. The bent arrow indicates the direction of transcription and the location of the putative promoters. The bars indicate the fragments used in various subclones (see Table 1). (B) Percentage of SasA$^+$ transformants from a variety of integration events. The percentage of SasA$^+$ transformants is calculated as the number of SasA$^+$ transformants divided by the total number of Km^r transformants tested for the SasA phenotype, multiplied by 100. The SasA$^+$ colonies are tan on CTT agar overlaid with 0.04% X-Gal, and the SasA$^-$ colonies are blue under these conditions. The number of transformants tested ranged between 128 and 1,181. The plasmids of the pHBK400 series contain inserts in the pBGS18 vector (Table 1). These plasmids integrate into the *sasA* locus. The results are listed in columns 1 and 2. The plasmids of the pHBK420 series contain inserts in the pLJS49 or pYC274 vector (Table 1). These plasmids integrate into the *M. xanthus* Mx8 phage attachment site (ATT). The results from integration of these plasmids are listed in column 3. The *asgB480* recipient in column 1 is DK6600, and the *asgB480 sasA1* recipient in columns 2 and 3 is DK6621. ND, not determined.

colonies which are blue when overlaid with X-Gal). These SasA$^-$ transformants are most likely a result of apparent gene conversion (42). A gene conversion rate of 10 to 25% is typical of these types of crosses in *M. xanthus* (39, 42).

Mapping the ends of the *sasA* locus and regenerating the mutant phenotype. To locate the ends of the *sasA* locus, a series of subclones were generated (Fig. 1A) and transferred into the *asgB480* parent strain DK6600, and their effect on the SasA phenotype was determined. The *sasA* mutants form small colonies which are blue when overlaid with X-Gal. They are easily distinguished from the large tan colonies of the parent. All of these plasmids integrate into the chromosome by a single recombination event, generating a tandem duplication of the region (Fig. 2). In this way, the integration of subclones containing both ends of the locus generates two complete copies of the locus. The integration of subclones containing either end of the locus generates one complete copy of the locus and one truncated copy. The integration of subclones containing internal fragments generates two incomplete copies of the locus. In this case, a copy of the locus truncated at the 3′ end is separated by vector sequences from another copy truncated at the 5′ end. Since the wild-type *sasA* locus is dominant over the mutant allele, SasA$^+$ strains are generated by the integration of subclones containing any end of the locus. SasA$^-$ strains are generated by the integration of subclones containing internal fragments. Figure 1B (column 1) reveals that the integration of four subclones (pHBK405, pHBK406, pDG408, and pDG409) into DK6600 resulted in no or very few SasA$^+$ transformants. These subclones must contain internal fragments. The integration of plasmids pHBK402 and pDG410, which contain inserts flanking the internal fragments, resulted in all SasA$^+$ transformants. These two subclones must each contain an end of the *sasA* locus.

The phenotypes of the double *sasA asgB480* mutant transformants, generated by the integration of fragments internal to the *sasA* locus, are identical in all respects tested to those of the original *sasA1 asgB480* mutant DK6621. This includes the ability of the mutant to hydrolyze X-Gal and form small glossy colonies. This suggests that the original *sasA1* mutation and the other 10 mutations generated by UV mutagenesis (17), which all give similar phenotypes, are null or loss-of-function mutations.

Mapping the *sasA1* mutation. To map the location of the *sasA1* mutation, various subclones of pHBK400 (Fig. 1A) were transferred into DK6621, the *sasA1 asgB480* mutant strain, and their effect on the SasA phenotype was determined. All of these plasmids recombine into the chromosome by a single recombination event, generating tandem copies of the *sasA* locus (Fig. 2). Any significant restoration of the SasA$^+$ phenotype requires the subclone to contain a wild-type *sasA* allele and at least one end of the locus. The integration of subclones containing the complete locus generates at least one wild-type copy of the locus. The majority of these transformants are SasA$^+$. A small percentage of SasA$^-$ transformants arise from apparent gene conversion and contain two mutant alleles. The integration of subclones containing either end of the locus and a wild-type *sasA* allele creates two types of duplications. In one case, the mutation and the truncated locus are on one side of the vector sequences, and a wild-type *sasA* locus is on the other side. These transformants are SasA$^+$. In the other case, the mutation and the truncation are separated, resulting in two mutant *sasA* loci. These transformants are SasA$^-$. The results shown in Fig. 1B (column 2) reveal that pHBK402 is the smallest subclone that contains one end of the *sasA* locus and the wild-type *sasA* allele. The approximately 50% restoration of the SasA$^+$ phenotype roughly maps the mutation to the region corresponding to the middle of the 1.5-kb insert.

The ability of subclones to produce a cytoplasmic product able to restore the SasA$^+$ phenotype to a *sasA1* mutant was tested by inserting different subclones (Fig. 1A) into the

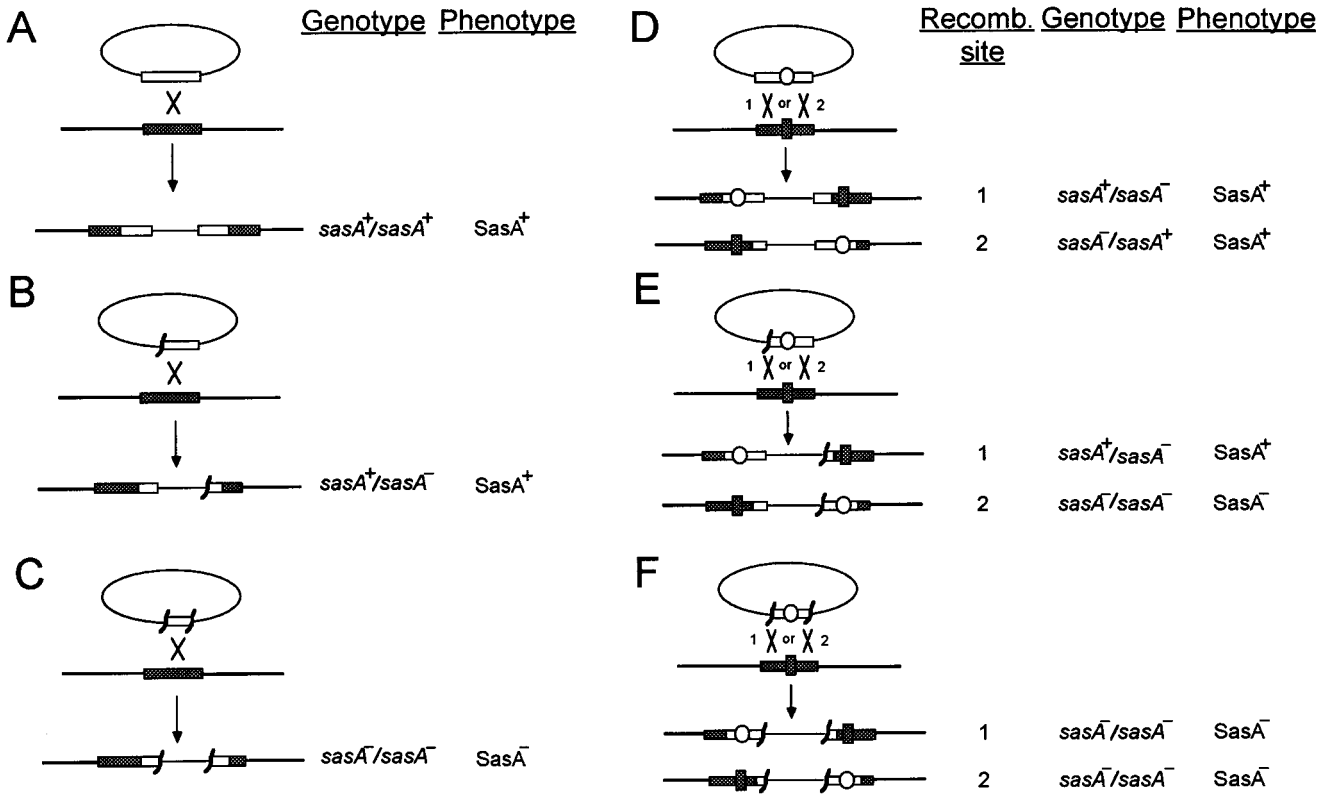

FIG. 2. Plasmid integration into the *M. xanthus* chromosome by homologous recombination at the *sasA* locus. The integration of plasmids each containing different amounts of the wild-type *sasA* locus into the *sasA*$^+$ *asgB480 M. xanthus* strain DK6600 (A through C) and into the *sasA1 asgB480* mutant DK6621 (D through F) was determined. (A and D) Integration of a plasmid containing a complete wild-type copy of the *sasA* locus. (B and E) Integration of a plasmid containing one end of the wild-type *sasA* locus. (C and F) Integration of a plasmid containing an internal fragment of the wild-type *sasA* locus. The open and shaded bars represent the same sequences originating from the plasmid and the chromosome, respectively. The curved line represents a truncated end of the *sasA* locus. The thin line represents vector sequences. The thick line represents the chromosome. The open circle represents the *sasA*$^+$ allele, and the shaded box represents the *sasA1* allele.

M. xanthus Mx8 phage attachment site. Any subclone that can restore the SasA$^+$ phenotype from this *trans* location is expected to contain a complete transcriptional unit. Surprisingly, the data shown in Fig. 1B (column 3) reveal that subclones smaller than those containing both ends of the *sasA* locus could restore the SasA$^+$ phenotype. The smallest subclone to restore the SasA$^+$ phenotype is pDG423. The ability of this subclone to restore the SasA$^+$ phenotype in *trans* suggests that it contains the *sasA* promoter and the complete open reading frame (ORF) which contains the mutation. These data, combined with the data from the integration of internal fragments (Fig. 1B, column 1), suggest that the *sasA1* mutation is nonpolar.

The *sasA* locus encodes a member of the family of ATP-binding cassette transporters. The nucleotide sequence of the 7-kb region containing the complete *sasA* locus was determined. Three ORFs were identified with the GCG Codonpreference program. The ORFs were given the gene designations *rfbA*, *B*, and *C*, based on their structural and functional similarities to the *rfb* loci of certain other gram-negative bacteria (3, 29, 44, 49). Figure 3 shows the DNA and deduced amino acid sequences of *rfbA* and *B*. The *rfbA* gene is predicted to encode a protein of 29,688 Da. It is predicted to start at nucleotide 862, which is 8 bp downstream of a possible ribosome-binding site (RBS), and to end at nucleotide 1644. A second possible translation start site in the same ORF is noted upstream, beginning at nucleotide 754. This is an unlikely start site because this additional coding region is enriched in rare codons, has a low G-C third-position codon bias (66.6%), and would encode an N-terminal extension of 32 amino acids in comparison to other similar proteins. In addition, a consensus RBS upstream of this start site is absent. The *rfbB* gene is predicted to encode a protein of 47,676 Da. It is predicted to start at nucleotide 1653, which is 8 bp downstream of a possible RBS, and to end at nucleotide 2966. A second possible translation start site in the same ORF is noted beginning at nucleotide 1665. This possible translation start site is not an optimal distance from a consensus RBS. The *rfbC* gene is predicted to encode a protein of 139,596 Da. It is predicted to start at nucleotide 3008, which is 7 bp downstream of a possible RBS, and to end at nucleotide 6835.

Due to the high G+C content (67.5%) of the *M. xanthus* chromosome (27), more than 87% of the nucleotides in the third codon position of each predicted ORF are expected to be a G or C (2). The G-C bias of the third codon position is 91.9% for *rfbA*, 87.0% for *rfbB*, and 87.7% for *rfbC*. The G+C content of each coding region is not significantly different from the G+C content of the genome. The total G+C content is 62.3% for *rfbA*, 66.2% for *rfbB*, and 70.3% for *rfbC*. Interestingly, two consensus −12 and −24 sequences characteristic of sigma 54-dependent promoters (28), such as the *M. xanthus* 4521 promoter (19), are present 147 and 100 bp upstream of the *rfbA* translation start site. No similarity to more standard promoter sequences is observed in this region.

Sequence analyses reveal structural similarities between the predicted *sasA* gene products and some deduced proteins required for lipopolysaccharide (LPS) O-antigen biosynthesis.

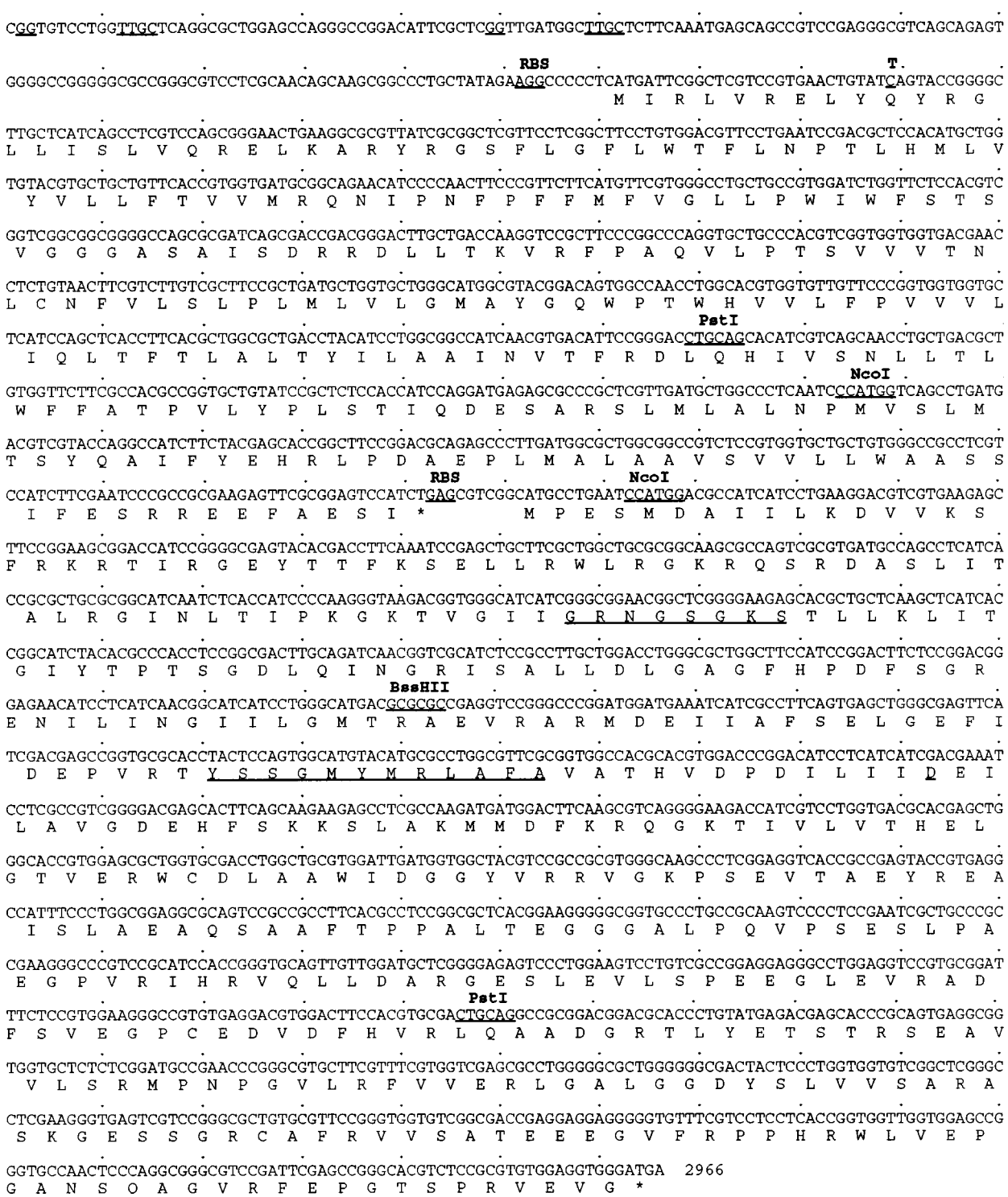

FIG. 3. Nucleotide sequence of the region of the *sasA* locus encoding the *rfbA* and *rfbB* genes. The DNA sequences and deduced amino acid sequences of the *rfbA* and *rfbB* genes are shown. The −12 and −24 sites of putative sigma 54-dependent promoters (28) are underlined. Translation stop codons are labeled by asterisks. The putative RBSs (45), the *sasA1* mutation, and the restriction enzyme recognition sites are underlined and labeled above the DNA sequence. The amino acids of the Walker ATP-binding site motif A site (GRNGSGKS) (46), the ATP-binding protein active-transport family signature (YSSGMYMRLAFA), and the conserved aspartate (D) of the Walker B site (46) are underlined.

The GCG Bestfit program calculates that the *rfbA* gene product is 21.5 to 31.0% identical to *rfb* gene products required for O-antigen biosynthesis in other gram-negative bacteria (3, 20, 44, 49). These deduced proteins are all predicted to be integral membrane domains of ATP-binding cassette (ABC) transporters. The predicted hydrophobicity of these proteins is very similar (Fig. 4). Each protein contains five or six hydrophobic regions. The Bestfit program calculates that the first 261 amino

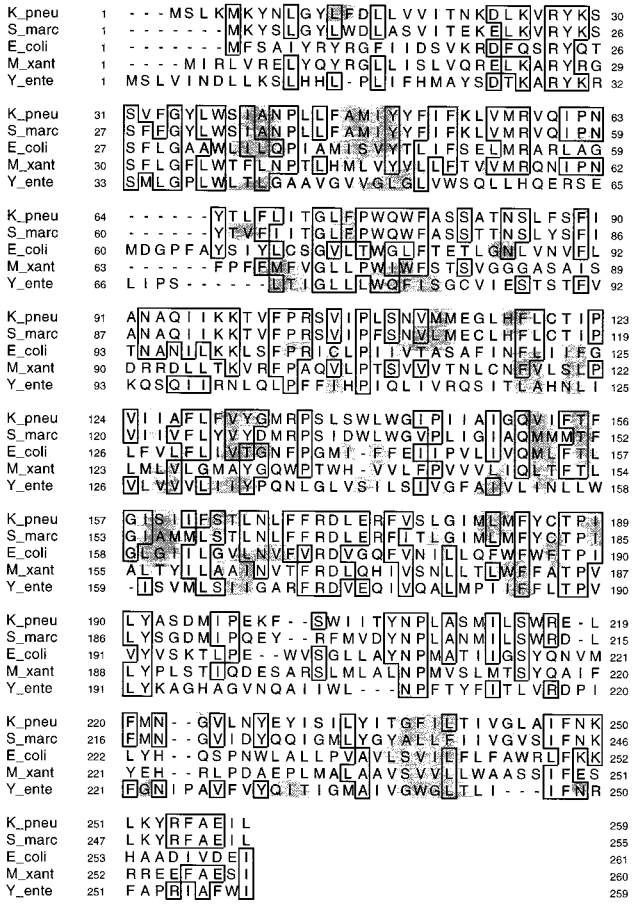

FIG. 4. Alignment and hydrophobicity of the deduced protein sequences of putative ABC transporter integral membrane domains required for O-antigen biosynthesis. The Pileup program of GCG version 8.0 was used to align the ORFs deduced from the *rfb* sequences of *Klebsiella pneumoniae* O1 (K. pneu) *rfbA* (3); *Serratia marcescens* O16 (S. marc) *rfbA* (44); *E. coli* O9 ORF261 (20); *M. xanthus* (M. xant) *rfbA*; and *Y. enterocolitica* O3 (Y. ente) *rfbD* (49). Three or more identical residues are boxed. The shaded areas represent hydrophobic regions.

acids of the *rfbB* gene product are 34.6 to 45.8% identical to *rfb* gene products predicted to be the ATPase domains of ABC transporters and also required for O-antigen biosynthesis (3, 20, 44, 49). An alignment of these proteins is shown in Fig. 5. Interestingly, the *M. xanthus rfbB* gene product and the *E. coli* ORF 431 have C-terminal extensions of 185 and 188 amino acids, respectively. These regions are not significantly identical. The GCG Motifs program identified in the *rfbB* gene product a Walker ATP-binding site motif (46) (Fig. 3). This includes both the A site, from amino acids 69 to 76, and the B site, consisting of an aspartate surrounded by a hydrophobic region, from amino acids 177 to 187. The ATP-binding proteins active-transport family signature from amino acids 157 to 168 was also identified.

The large ORF of *rfbC* shows only limited identity to proteins in the databases. The most significant match is to the *Y. enterocolitica* O3 *rfbH* gene product (49). The Tfasta program indicates an identity of 33.8% over a region of 358 amino acids between amino acid 894 and amino acid 1254 in the C-terminal quarter of this predicted 1,276-amino-acid *M. xanthus* protein. The *Y. enterocolitica* O3 *rfbH* gene product of 421 amino acids is required for O-antigen biosynthesis, but its function is unclear (49).

The *sasA1* allele encodes a nonsense mutation. The DNA alteration causing the *sasA1* mutation was determined by sequencing PCR products generated with chromosomal DNA from the *sasA1 asgB480* mutant DK6621 as the template. The *sasA1* mutation is a transition of a C to a T at nucleotide 889, located in the beginning of the *rfbA* coding region (Fig. 3). This results in a change of a glutamine at amino acid 46 to an amber stop codon. The resulting *rfbA* gene product will be truncated and most likely have lost its ability to function.

A wild-type *sasA* locus is required for O-antigen biosynthesis. To determine if the *sasA* gene products are functionally as well as structurally related to those required for O-antigen biosynthesis, we tested the reactivity of the *sasA1 asgB480* mutant DK6621 to antibodies directed against *M. xanthus* LPS (12). The immunoblot analysis (Fig. 6) revealed that this mutant reacted weakly with MAbs (kindly provided by M. Dworkin) against *M. xanthus* O-antigen and purified LPS. This mutant reacted strongly with MAbs directed against *M. xanthus* LPS core. The wild-type strain, DK6620, and the *asgB480* parent, DK6600, reacted strongly with all of the MAbs. These data indicate that a wild-type *sasA* locus is required for the biosynthesis of *M. xanthus* O-antigen.

Production of extracellular A signal is independent of the *sasA* locus. The *M. xanthus rfbA*, *B*, and *C* genes are related to ABC transporters that function as exporters. To address the possibility that the *sasA* locus plays a role in the production of extracellular A signal, the A-signal activity in supernatants of developing wild-type and *sasA* mutants was measured. In all cases, the *sasA* and *sasA*$^+$ isogenic strains had essentially the same level of extracellular A signal. The A-signal units (ASU) measured in the supernatants of the *sasA* mutant DK6639 and its isogenic wild-type strain DK6638 were 20.3 and 22.1 ASU/ml, respectively. The A-signal units measured in the supernatants of the *sasA* mutant DK6641 and its isogenic wild-type strain DK6640 were 12.6 and 12.5 ASU/ml, respectively. Previous data (17) also showed that the A-signal activity level of *sasA1 asgB480* mutants (0.43 ASU/ml) is not significantly higher than that of its *asgB480* parent (0.2 ASU/ml). All of these data indicate that the production of extracellular A signal is independent of the *sasA* locus. In fact, the A-signal activity levels of the *sasA1 asgB480* mutant show that the increase in 4521 expression in the *sasA* mutant strains is not due to an increase in extracellular A-signal production.

DISCUSSION

The wild-type *M. xanthus sasA* locus has been cloned, sequenced, and determined to function in O-antigen biosynthesis. Each of the *M. xanthus rfbABC* gene products has regions of identity with *rfb* gene products involved in O-antigen biosynthesis in certain other gram-negative bacteria (3, 20, 44, 49). These gram-negative bacteria appear to use an ABC transporter to export the O-antigen from the cytoplasm (3, 49). This group of ABC exporters are members of a subfamily defined by Reizer et al. (34) as ABC-2. Interestingly, similar proteins have not been identified in *Salmonella* strains (20, 47).

The *rfbAB* gene products are predicted to encode an ABC transporter (9). It is most likely that RfbA and RfbB each form homodimers which function together as a transporter. RfbA should provide a channel, and RfbB should couple the hydrolysis of ATP to the transport of molecules through this channel. Both elements should be necessary for function. It is likely that *M. xanthus* O-antigen is polymerized within the cytoplasm and transported by this ABC transporter across the cytoplasmic membrane to the periplasmic space, where ligation to lipid A-core occurs.

```
K_pneu   1  - - - MEPVINFSNVTKEYPLYHHIG - - SGIKDLV 28
S_marc   1  - - - MSVAIEFKNVTKRYPLYHHIG - - SGIKELI 28
M_xant   1  MPESMDAIILKDVVKSFRKRTIRGEYTTFKSEL 33
E_coli   1  - - - - - MSIKVQHVGKAYKYYP - - - - - SKWSRVI 23
Y_ente   1  - - - - MTSLIFKNVTMSYPIYNAHSQ - - SLRNQL 27

K_pneu  29  FHPKRAFQLLKGRK - - - YL - AIEDISFTVAKGE 57
S_marc  29  FNPRRALSLLSGRS - - - YL - AIEDICFQVQKGE 57
M_xant  34  LRWLRGKRQSRDAS - - - LITALRGINLTIPKGK 63
E_coli  24  EKLLPGDKPRHSKK - - - WV - - LKDINFSIEPGE 51
Y_ente  28  VRVSTGGRIGGSRGEVVTVTALDNISFELNSGD 60

K_pneu  58  AVALIGRNGAGKSTSLGLVAGVIKPTKGSVTTH 90
S_marc  58  SVALIGRNGAGKSTSLGLVAGVMKPSSGSVHVV 90
M_xant  64  TVGIIGRNGSGKSTLLKLITGIYTPTSGDLQIN 96
E_coli  52  AVGIVGVNGAGKSTLLKLLTGTTQPTKGSIEIQ 84
Y_ente  61  SVGLIGHNGAGKSTLLRTMAGIYPASSGEIIRE 93

K_pneu  91  GRVASMLELGGGFHPELTGRENIYLNATLLGLR 123
S_marc  91  GRVASMLELGGGFHPELTGRENIRLNATLLGLR 123
M_xant  97  GRISALLDLGAGFHPDFSGRENILINGIILGMT 129
E_coli  85  GRVAALLELGMGFHPDFTGRQNVYMSGLMMGLG 117
Y_ente  94  GSVATVFELGAGMDPELSGYENIMRMLLLLGNS 126

K_pneu 124  RKEVQQRMERIIEFSELGEFIDEPIRVYSSGML 156
S_marc 124  RKELKQRLDKIIEFSELGEFIDEPIRVYSSGML 156
M_xant 130  RAEVRARMDEIIAFSELGEFIDEPVRTYSSGMY 162
E_coli 118  REEIERLMPEIEAFADIGDYIEEPVRIYSSGMQ 150
Y_ente 127  VASAKSKIPEIEEFCELGDFLVLPVRTYSSGMT 159

K_pneu 157  AKLGFSVISQVEPDILIIDEVLAVGDISFQAKC 189
S_marc 157  AKLGFSVITQVDPDILIIDEVLAVGDIAFQRKC 189
M_xant 163  MRLAFAVATHVDPDILIIDEILAVGDEHFSKKS 195
E_coli 151  MRLAFAVATASRPDILIVDEALSVGDSRFQAKC 183
Y_ente 160  MRLMFAVATSMRPEILLIDEMFGTGDAAFQEKA 192

K_pneu 190  IKTIREFKKKGVTILFVSHNMSDVERICDRVVW 222
S_marc 190  IKTINEFKSKGVTILFVSHNLEDVEKICDKVIW 222
M_xant 196  LAKMMDFKRQGKTIVLVTHELGTVERWCDLAAW 228
E_coli 184  YARIADFKEQGTTLLLVSHSAGDIVKHCDRAIF 216
Y_ente 193  EKRMRDWIAGSDIFVFASHDRSLIKKLCNRIFR 225

K_pneu 223  IENHRLREIGSAERIIELYKQAMA - - - - - - - - - 246
S_marc 223  IENHKMKAMGDAHSIISQYKTAMA - - - - - - - - - 246
M_xant 229  IDGGYVRRVGKPSEVTAEYREAISLAEAQSAAF 261
E_coli 217  LKNGDICMDGTARDVTNRYLDELFGKPDKDSAT 249
Y_ente 226  LEHGLIYEESMDIL - - - - - - - - - - - - - - - - - - - 239
```

FIG. 5. Alignment of the deduced protein sequences of putative ABC transporter ATPase domains required for O-antigen biosynthesis. The Pileup program of GCG version 8.0 was used to align the ORFs deduced from the *rfb* sequences of *K. pneumoniae* O1 (K. pneu) *rfbB* (3); *S. marcescens* O16 (S. marc) *rfbB* (44); *M. xanthus* (M. xant) *rfbB*; *E. coli* O9 ORF431 (20); and *Y. enterocolitica* O3 (Y. ente) *rfbE* (49). The shaded areas represent three or more identical residues. The complete ORFs of *K. pneumoniae* O1 RfbB, *S. marcescens* O16 RfbB, and *Y. enterocolitica* O3 RfbE are shown. The *M. xanthus* RfbB and *E. coli* ORF431 sequences continue for another 185 and 188 amino acids, respectively.

The *sasA1* mutation is a nonsense mutation which maps to the beginning of the *rfbA* gene. Interestingly, the wild-type *rfbA* alone, when present at the Mx8 phage attachment site, can restore the SasA$^+$ phenotype to a *sasA1* mutant. This suggests that the *sasA1* mutation is nonpolar. The possibility that *rfbB* has a separate promoter is unlikely from the mapping data, which suggest that the 7-kb region is one transcriptional unit. It is most likely that the *rfbB* gene is also required for O-antigen biosynthesis. At least one *sasA* point mutation appears to map to this gene.

The *rfbC* gene appears to be required for *M. xanthus* O-antigen biosynthesis. Integration of fragments internal to the *rfbC* gene into the chromosome of a *sasA*$^+$ strain generates mutants with the same phenotypes as those of the *sasA1* mutant (Fig. 1B, column 1). In addition, cotransductional mapping of the original point mutants (17) indicates that at least two other *sasA* mutations with phenotypes identical to *sasA1* map to *rfbC*. The *rfbC* gene, which is almost 4 kb, is very large for a bacterial gene. It is striking that only the C-terminal quarter of the predicted protein has significant identity to one other protein, the *Y. enterocolitica* O3 *rfbH* gene product (49). This *Y. enterocolitica* gene product is involved in O-antigen biosynthesis, but its specific function is currently unknown. Further analysis is required to understand the function of *rfbC* in *M. xanthus* O-antigen biosynthesis.

M. xanthus LPS contains three distinct regions: lipid A, which forms the outer leaflet of the outer membrane bilayer; core, which contains a chain of carbohydrates attached to lipid A; and O-antigen, which contains a variable number of repeating oligosaccharide units and extends outward from the core region (10). The carbohydrate content of *M. xanthus* LPS varies between growing and developing cells (30, 43). In addition, methylation of the *M. xanthus* LPS occurs during the early stages of development (29, 30).

M. xanthus mutants deficient in O-antigen biosynthesis have previously been isolated (11). Five Tn*5* insertion mutations map to three unlinked loci (5). The strains containing these insertions share certain characteristics with the *sasA* mutants (11, 17); their colonies are small and their developmental cycle is delayed. However, these mutants, unlike the *sasA* mutants, are described as being deficient in *M. xanthus* single-cell movement (adventurous motility) and eventually forming wild-type fruiting bodies. To address the locus specificity of A-signal-independent 4521 developmental expression, the level of 4521 expression in these backgrounds will be measured. It will also be interesting to examine the relationship of these O-antigen biosynthesis loci to the *sasA* locus.

The connection between the absence or reduction in the level of O-antigen and the increase in expression of 4521 developmental expression remains obscure. However, the evidence suggests that the *sasA* mutations increase 4521 developmental expression by bypassing the A-signal/cell density control of 4521 gene expression while maintaining the starvation control. Expression of 4521 in the *sasA1 asgB480* mutant DK6621 clearly responds to starvation by increasing expression at 2 h into development (17). In addition, Singer and Kaiser (40) have recently shown that 4521 expression levels reach 60% of developmental levels during growth when the apparent starvation signal (p)ppGpp is supplied.

Interestingly, the *sasA* mutations affect the expression of only a specific subset of A-signal-dependent genes (17). The expression of this subset of genes is differentially affected. The expression of two genes, 4521 and 4445, is increased in response to the *sasA1* mutation. In contrast, the expression of two other genes, 4442 and 4427, is decreased in response to the *sasA1* mutation. The *sasA* mutations may bypass the A-signal/cell density control of 4521 gene expression through the cytoplasmic accumulation of intermediates in O-antigen biosynthesis or a change in cell surface properties.

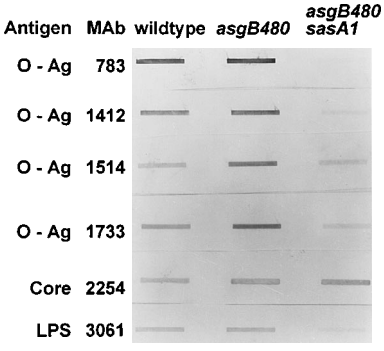

FIG. 6. Immunoblot analysis of whole *M. xanthus* cells reacted with MAbs against *M. xanthus* LPS. Approximately 10^6 exponentially growing *M. xanthus* cells were resuspended in TBS buffer, transferred to a nitrocellulose membrane, and reacted with the MAbs against the *M. xanthus* antigen listed. The MAbs (12) were generously provided by M. Dworkin. Strain DK6620 is the wild type, DK6600 is the *asgB480* parent, and DK6621 is the *sasA1 asgB480* mutant. O-Ag, O-antigen.

ACKNOWLEDGMENTS

We thank D. Kaiser, in whose laboratory this work was initiated, and A. Muhammed, L. Armitige, T. A. Dang, D. S. Lim, and Y. Wu for excellent technical assistance. We also thank C. Yang for making pCY274 available to us and S. Hull and W. Margolin for comments on the manuscript. M. Dworkin very generously provided the monoclonal antibodies used in this study.

This investigation was supported by Public Health Service grant GM47444 to H.K. from the National Institutes of Health.

REFERENCES

1. **Altschul, S. F., W. Gish, W. Miller, E. W. Myers, and D. J. Lipman.** 1990. Basic local alignment search tool. J. Mol. Biol. **215:**403–410.
2. **Bibb, M. J., P. R. Findlay, and M. W. Johnson.** 1984. The relationship between base composition and codon usage in bacterial genes and its use for the simple and reliable identification of protein-coding sequences. Gene **30:** 157–166.
3. **Bronner, D., B. R. Clarke, and C. Whitfield.** 1994. Identification of an ATP-binding cassette transport system required for translocation of lipopolysaccharide O-antigen side-chains across the cytoplasmic membrane of *Klebsiella pneumoniae* serotype O1. Mol. Microbiol. **14:**505–519.
4. **Casadaban, M. J., and S. N. Cohen.** 1980. Analysis of gene control signals by DNA fusion and cloning in *E. coli*. J. Mol. Biol. **138:**179–207.
5. **Chen, H. W., A. Kuspa, I. M. Keseler, and L. J. Shimkets.** 1991. Physical map of the *Myxococcus xanthus* chromosome. J. Bacteriol. **173:**2109–2115.
6. **Devereux, J., P. Haeberli, and O. Smithies.** 1984. A comprehensive set of sequence analysis programs for the VAX. Nucleic Acids Res. **12:**387–395.
7. **Downard, J., S. V. Ramaswamy, and K. S. Kil.** 1993. Identification of *esg*, a genetic locus involved in cell-cell signaling during *Myxococcus xanthus* development. J. Bacteriol. **175:**7762–7770.
8. **Dworkin, M., and D. Kaiser.** 1993. Myxobacteria II. American Society for Microbiology, Washington, D.C.
9. **Fath, M. J., and R. Kolter.** 1993. ABC transporters: bacterial exporters. Microbiol. Rev. **57:**995–1017.
10. **Fink, J. M., and J. F. Zissler.** 1989. Characterization of lipopolysaccharide from *Myxococcus xanthus* by use of monoclonal antibodies. J. Bacteriol. **171:** 2028–2032.
11. **Fink, J. M., and J. F. Zissler.** 1989. Defects in motility and development of *Myxococcus xanthus* lipopolysaccharide mutants. J. Bacteriol. **171:**2042–2048.
12. **Gill, J. S., and M. Dworkin.** 1986. Cell surface antigens during submerged development of *Myxococcus xanthus* examined with monoclonal antibodies. J. Bacteriol. **168:**505–511.
13. **Gill, R. E., M. G. Cull, and S. Fly.** 1988. Genetic identification and cloning of a gene required for developmental cell interactions in *Myxococcus xanthus*. J. Bacteriol. **170:**5279–5288.
14. **Gulati, P., D. Xu, and H. B. Kaplan.** 1995. Identification of the minimum regulatory region of a *Myxococcus xanthus* A-signal-dependent developmental gene. J. Bacteriol. **177:**4645–4651.
15. **Hagen, D. C., A. P. Bretscher, and D. Kaiser.** 1978. Synergism between morphogenetic mutants of *Myxococcus xanthus*. Dev. Biol. **64:**284–296.
16. **Hanahan, D.** 1983. Studies on transformation of *Escherichia coli* with plasmids. J. Mol. Biol. **166:**557–580.
17. **Kaplan, H. B., A. Kuspa, and D. Kaiser.** 1991. Suppressors that permit A-signal-independent developmental gene expression in *Myxococcus xanthus*. J. Bacteriol. **173:**1460–1470.
18. **Kashefi, K., and P. L. Hartzell.** 1995. Genetic suppression and phenotypic masking of a *Myxococcus xanthus frzF*$^-$ defect. Mol. Microbiol. **15:**483–494.
19. **Keseler, I. M., and D. Kaiser.** 1995. An early A-signal-dependent gene in *Myxococcus xanthus* has a σ^{54}-like promoter. J. Bacteriol. **177:**4638–4644.
20. **Kido, N., V. Torgov, T. Sugiyama, K. Uchiya, H. Sugihara, T. Komatsu, K. Kato, and K. Jann.** 1995. Expression of the O9 polysaccharide of *Escherichia coli*: sequencing of the *E. coli* O9 *rfb* gene cluster, characterization of mannosyl transferases, and evidence for an ATP-binding cassette transport system. J. Bacteriol. **177:**2178–2187.
21. **Kroos, L., A. Kuspa, and D. Kaiser.** 1986. A global analysis of developmentally regulated genes in *Myxococcus xanthus*. Dev. Biol. **117:**252–266.
22. **Kuspa, A., and D. Kaiser.** 1989. Genes required for developmental signalling in *Myxococcus xanthus*: three *asg* loci. J. Bacteriol. **171:**2762–2772.
23. **Kuspa, A., L. Kroos, and D. Kaiser.** 1986. Intercellular signaling is required for developmental gene expression in *Myxococcus xanthus*. Dev. Biol. **117:** 267–276.
24. **Kuspa, A., L. Plamann, and D. Kaiser.** 1992. Identification of heat-stable A-factor from *Myxococcus xanthus*. J. Bacteriol. **174:**3319–3326.
25. **Kuspa, A., L. Plamann, and D. Kaiser.** 1992. A-signalling and the cell density requirement for *Myxococcus xanthus* development. J. Bacteriol. **174:**7360–7369.
26. **Kustu, S., E. Santero, J. Keener, D. Popham, and D. Weiss.** 1989. Expression of σ^{54} (*ntrA*)-dependent genes is probably united by a common mechanism. Microbiol. Rev. **53:**367–376.
27. **Mesbah, M., U. Premachandran, and W. B. Whitman.** 1989. Precise measurement of the G+C content of deoxyribonucleic acid by high-performance liquid chromatography. Int. J. Syst. Bacteriol. **39:**159–167.
28. **Morett, E., and B. Martin.** 1989. *In vivo* studies of the interaction of RNA polymerase-σ^{54} with the *Klebsiella pneumoniae* and *Rhizobium meliloti nifH* promoters. J. Mol. Biol. **210:**65–77.
29. **Panasenko, S. M.** 1985. Methylation of macromolecules during development in *Myxococcus xanthus*. J. Bacteriol. **164:**495–500.
30. **Panasenko, S. M., B. Jann, and K. Jann.** 1989. Novel change in the carbohydrate portion of *Myxococcus xanthus* lipopolysaccharide during development. J. Bacteriol. **171:**1835–1840.
31. **Plamann, L., J. M. Davis, B. Cantwell, and J. Mayor.** 1994. Evidence that *asgB* encodes a DNA-binding protein essential for growth and development of *Myxococcus xanthus*. J. Bacteriol. **176:**2013–2020.
32. **Plamann, L., A. Kuspa, and D. Kaiser.** 1992. Proteins that rescue A-signal-defective mutants of *Myxococcus xanthus*. J. Bacteriol. **174:**3311–3318.
33. **Plamann, L., Y. Li, B. Cantwell, and J. Mayor.** 1995. The *Myxococcus xanthus asgA* gene encodes a novel signal transduction protein required for multicellular development. J. Bacteriol. **177:**2014–2020.
34. **Reizer, J., A. Reizer, and M. H. Saier.** 1992. A new subfamily of bacterial ABC-type transporter systems catalyzing export of drugs and carbohydrates. Protein Sci. **1:**1326–1332.
35. **Sambrook, J., E. F. Fritsch, and T. Maniatis.** 1989. Molecular cloning: a laboratory manual, 2nd ed. Cold Spring Harbor Laboratory Press, Cold Spring Harbor, N.Y.
36. **Sanger, F., S. Nicklen, and A. R. Coulson.** 1977. DNA sequencing with chain-terminating inhibitors. Proc. Natl. Acad. Sci. USA **74:**5463–5467.
37. **Shimkets, L. J.** 1990. Social and developmental biology of the myxobacteria. Microbiol. Rev. **54:**473–501.
38. **Shimkets, L. J., and S. J. Asher.** 1988. Use of recombination techniques to examine the structure of the *csg* locus of *Myxococcus xanthus*. Mol. Gen. Genet. **211:**63–71.
39. **Shimkets, L. J., R. E. Gill, and D. Kaiser.** 1983. Development cell interactions in *Myxococcus xanthus* and the *spoC* locus. Proc. Natl. Acad. Sci. USA **80:**1406–1410.
40. **Singer, M., and D. Kaiser.** 1995. Ectopic production of guanosine penta- and tetraphosphate can initiate early developmental gene expression in *Myxococcus xanthus*. Genes Dev. **9:**1633–1644.
41. **Spratt, B. G., P. J. Hedge, S. Heesen, A. Edelman, and J. K. Broome-Smith.** 1986. Kanamycin-resistant vectors that are analogues of plasmids pUC8, pUC9, pEMBL8, and pEMBL9. Gene **41:**337–342.
42. **Stephens, K., and D. Kaiser.** 1987. Genetics of gliding motility in *Myxococcus xanthus*: molecular cloning of the *mgl* locus. Mol. Gen. Genet. **207:**256–266.
43. **Sutherland, I. W.** 1976. Novel surface polymer changes in development of *Myxococcus* spp. Nature (London) **259:**46–47.
44. **Szabo, M., D. Bronner, and C. Whitfield.** 1995. Relationships between *rfb* gene clusters required for biosynthesis of identical D-galactose-containing O antigens in *Klebsiella pneumoniae* serotype O1 and *Serratia marcescens* serotype O16. J. Bacteriol. **177:**1544–1553.
45. **von Heijne, G.** 1987. Sequence analysis in molecular biology. Academic Press, Inc., New York.
46. **Walker, J. E., M. Sarste, M. J. Runswick, and N. J. Gay.** 1982. Distantly related sequences in the α- and β-subunits of ATP synthase, myosin, kinases and other ATP-requiring enzymes and a common nucleotide binding fold. EMBO J. **1:**945–951.
47. **Whitfield, C., and M. A. Valvano.** 1993. Biosynthesis and expression of the cell-surface polysaccharides in Gram-negative bacteria. Adv. Microbiol. Phys. **35:**135–246.
48. **Yanisch-Perron, C., J. Vieira, and J. Messing.** 1985. Improved M13 phage cloning vectors: nucleotide sequences of the M13mp18 and pUC19 vectors. Gene **33:**103–119.
49. **Zhang, L., A. Al-Hendy, P. Toivan, and M. Skurnik.** 1993. Genetic organization and sequence of the *rfb* gene cluster of *Yersinia enterocolitica* serotype O:3: similarities to the dTDP-L-rhamnose biosynthesis pathway of *Salmonella* and to the bacterial polysaccharide transport systems. Mol. Microbiol. **9:**309–321.